PRAMANA
—journal of
physics



Vol. 53, No. 1,
July 1999
pp. 25–35

# Surface controlled nematic bistability*

I DOZOV and G DURAND
Laboratoire de Physique des Solides, Bat 510, Centre Universitaire, 91405 Orsay Cedex, France

**Abstract.** One discusses phenomenologically the statics and dynamics of surface anchoring of nematic liquid crystals. In statics, for symmetrical situations, one can induce, under the action of an external field, a surface breaking with a bifurcation between two opposite orientations of the director. In dynamics, one shows that the surface director relaxation is intrinsically fast, and accompanied by a transient surface shear flow. In thin cells with planar anchorings, filled by cyanobiphenyl materials which orient normal to the plates under a strong electric field, there are now two effects which couple the relaxation of the surface director: a static one, which favors parallel orientation and a uniform cell texture, and a transient dynamical coupling from the surface flow, which forces $\pi$-twisted texture. With suitable electric signals, one can control the surface bifurcations to give at will one of these two bistable textures. Results are presented which show that these mechanisms could lead to a new class of surface controlled, fast nematic bistable displays.

**Keywords.** Bistability nematic; surface anchoring; liquid crystal displays.

**PACS Nos 68.45-V; 61.30.Gd; 78.20.Jq**

## 1. Introduction

Liquid crystals, and in particular nematics, are easily distorted by weak electric fields, leading to electro-optic effects widely used in display technologies. Traditional nematic displays are bulk *monostable* devices: the texture changes take place in the volume of the display, at fixed surface anchoring. When the field is shut off, the pixel goes back to the unique equilibrium stable structure. A serious improvement of the performance is expected for bistable devices, having two distinct textures, stable in the absence of a field, but electrically switchable. In principle, bistability enables infinitely long memory time, infinite multiplexability (and high resolution), and low power consumption. The well-known 'active' matrix displays are one example of bistable devices. Their bistability is not intrinsic, but is due to active elements, thin film transistors (TFT) or diodes, one per pixel, which make the display very complex and expensive. Several 'passive' bulk devices with intrinsic bistability have also been proposed. They are switched by the propagation of defects [1] or by continuous bulk deformation [2], in both cases too slow for video rate applications.

Passive surface controlled bistable switching has been proposed and realized for smectic C* [3] and nematic [4] liquid crystals. These devices use two physically different

* Reproduced from '*Liquid Crystals Today*' (Vol. 8, p. 1–7, 1998) by permission from Taylor and Francis.

anchoring directions on the plates. They are fast, but depend on complex 'bistable' alignments. The drawback of the ferroelectric SmC* is its large sensitivity to mechanical shocks, leading to irreversible stress damage. In the nematic case, which is mechanically stable, the main difficulty is to realize the bistable alignments.

Recently we have proposed a new kind of passive surface-controlled nematic display with bistable textures, switched by breaking *simple* anchorings [5–9]. After the surface relaxation, the surface director can be $\mathbf{n}_s$ or $-\mathbf{n}_s$, giving two different bulk textures. These two bistable textures differ drastically in their optical properties, giving good contrast and a wide viewing angle. The proposed device is technologically simple, with trivial surface planar alignments. By using a nematic material, the display is unaffected by mechanical or thermal perturbations. The switching by breaking surface anchoring is very fast and can be controlled by pulses of a few microseconds duration.

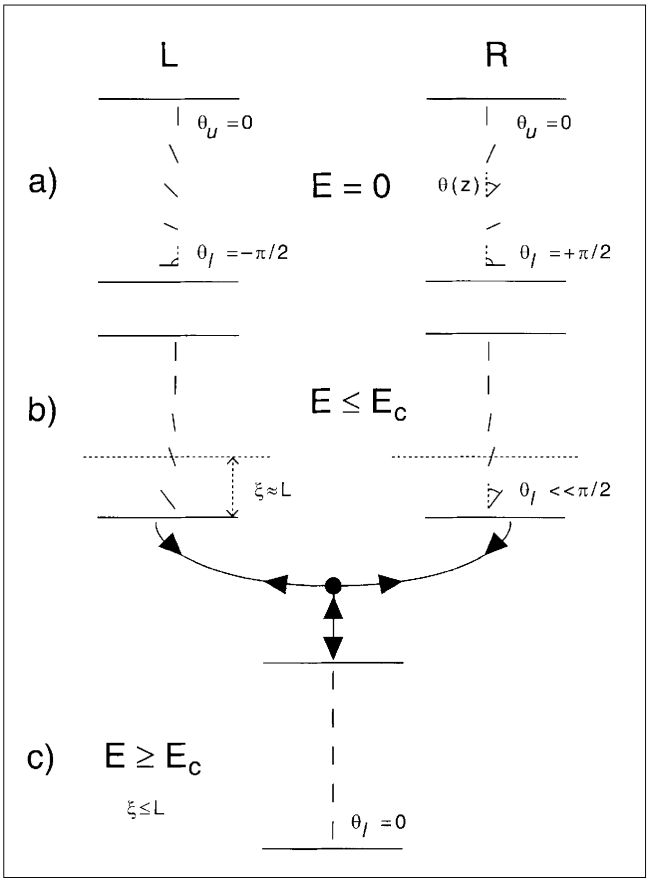


**Figure 1.** Breaking of the anchoring in a hybrid nematic cell. Left (L) and Right (R) columns present the two degenerate textures. (**a**) $E = 0$. Uniform distortion in the bulk. (**b**) $E < E_c$. Distortion near the planar plate. Surface director tilted from the easy axis. (**c**) $E > E_c$. The lower plate anchoring is broken, the sample is homeotropic.

## 2. Breaking of the surface anchoring

Imagine a hybrid nematic cell (figure 1) with positive dielectric anisotropy $\varepsilon_a > 0$, under an electric field $E$ normal to the plates. The nematic director is defined as $\mathbf{n} = (\sin\theta, 0, \cos\theta)$. At the upper plate the alignment is homeotropic ($\theta_u = 0$), stabilized by the field. On the lower plate it is planar without pretilt ($\theta_l = \pm\pi/2$, due to the equivalence of $\mathbf{n}_l$ and $-\mathbf{n}_l$). Without a field two different uniformly distorted textures can be realized (figure 1a, left and right, for simplicity we suppose $K_1 = K_3 = K$). Under an applied field, the distortion is concentrated in a region of thickness $\xi$ around the planar plate, $\xi = (4\pi K/\epsilon_a)^{1/2}/E$ being the electric field coherence length. We suppose the Rapini–Papoular form of the anchoring energy $W_a = (1/2)(K/L)\cos^2\theta_l$, where $L \sim 1000$ Å is the surface extrapolation length. The total dielectric torque $\Gamma_d = (K/\xi)\sin\theta_l$ is transmitted to the lower plate, competing against the surface anchoring torque $\Gamma_s = (1/2)(K/L)\sin(2\theta_l)$. For weak fields ($\xi \gg L$), the surface orientation remains $\theta_l \cong \pm\pi/2$, but when the field increases ($\xi > L$), the surface orientation changes ($\mid \theta_l \mid \ll \pi/2$, figure 1b). Finally, at the critical field $E_c$, defined by $\xi_c = L$, the sample becomes completely homeotropic (figure 1c). For 5CB aligned on SiO, $E_c$ is about 7–10 V μm$^{-1}$ [4, 10]. The anchoring is now 'broken' [11, 12] and the surface orientation $\theta_l$ corresponds to a *minimum* of the bulk energy (electric plus elastic) and to a *maximum* of the surface anchoring energy. This surface 'breaking' is a second order texture transition (figure 2): above $E_c$ the sample is homeotropic ($\theta_l = 0$), below $E_c$ two degenerate solutions exist for the surface orientation ($\mid \theta_l \mid < \pi/2$). For reasons of symmetry, this transition is possible only in the case of *strictly* planar anchoring. At $E = E_c$ the system passes through a 'bifurcation point', connecting the high field $\theta_l = 0$ texture with the two low field solutions. At the bifurcation the surface director can go back towards the equilibrium planar state in two different ways. It becomes very sensitive to perturbations at the bifurcation, where the surface susceptibility diverges. Weak effects would be sufficient to switch the system to the positive or the negative branch of figure 2, independently of the (now forgotten) initial texture.

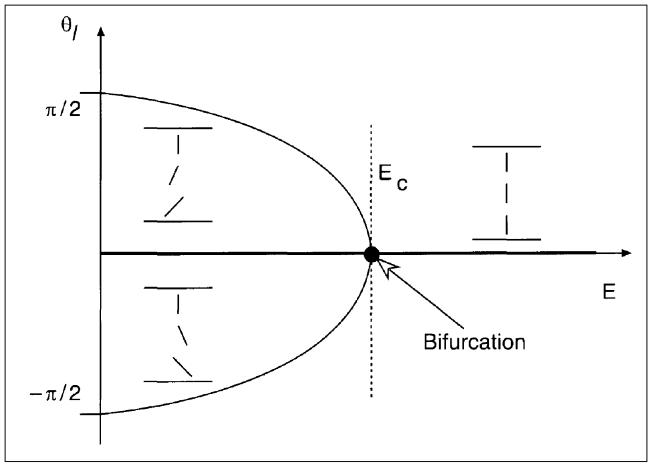


**Figure 2.** Anchoring-breaking transition under an electric field. The two symmetric branches at $E < E_c$ join at the bifurcation point, for $\xi_c = L$.

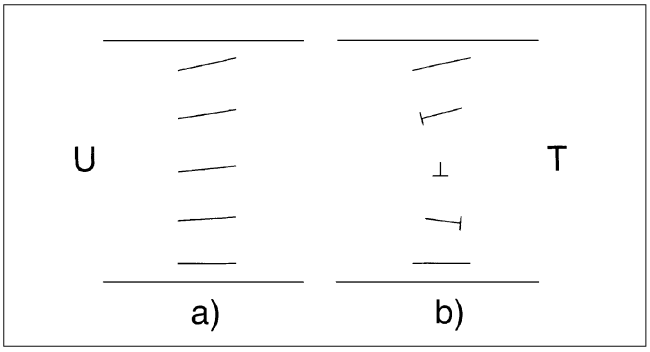


**Figure 3.** Topologically distinct bistable textures: (**a**) quasi-uniform $U$; (**b**) half-turn twisted $T$.

## 3. Bistable bulk textures

The two bulk bistable hybrid textures (figure 1a) have almost the same optical properties and can hardly be useful for displays, except for writing and erasing surface defects [13]. Can we create with the surface bifurcation two bulk textures with drastically different optical properties? Let the lower plate present planar alignment with moderate anchoring strength. The upper plate has a very strong planar or slightly tilted anchoring: the alignment on this plate will never break. An infinite number of different textures can be realized with these anchorings, with the total distortion in the cell equal to $\pm m\pi$ (an integral number of half-turns). The lowest energy texture is the quasi uniform state $U$ of figure 3a. Among the distorted textures the lowest energy belongs to the half-turn twisted state $T$ (right or left, $m = \pm 1$), presented in figure 3b. Topologically, for fixed boundaries, $T$ and $U$ are two distinct states. There is no transition between them by continuous bulk deformation, and they are toplogically stable. However, a local transition between the $U$ and $T$ textures is possible by propagation of disclination lines of strength $S = \pm 1/2$. These defects could be induced for instance from cell filling imperfections. The distortion energy difference between $U$ and $T$ forces the defects propagation. Locally, after the defect action, the system goes from $T$ to $U$ state, 'tunneling' through the energy barrier. To avoid this parasitic local switching and to obtain true bistability, we need to prevent the propagation of disclination lines. One way to do this is to 'chiralize' the nematic, equalizing the energy of the two textures. Another way is to pin the bulk lines on the surfaces, as wall defects. This can sometimes be achieved by applying short and strong electric pulses, or even spontaneously [6, 7], and in this way we have stabilized the textures $U$ and $T$ for several months, achieving true bistability of the two states.

## 4. Switching by surface anchoring breaking

Starting from $U$ or $T$ (figure 3) we apply an electric field $E > E_c$ strong enough to break the lower plate anchoring. The cell is now almost homeotropic (figure 4a), except for a thin layer close to the strongly anchored upper plate: the initial texture is forgotten. If we turn

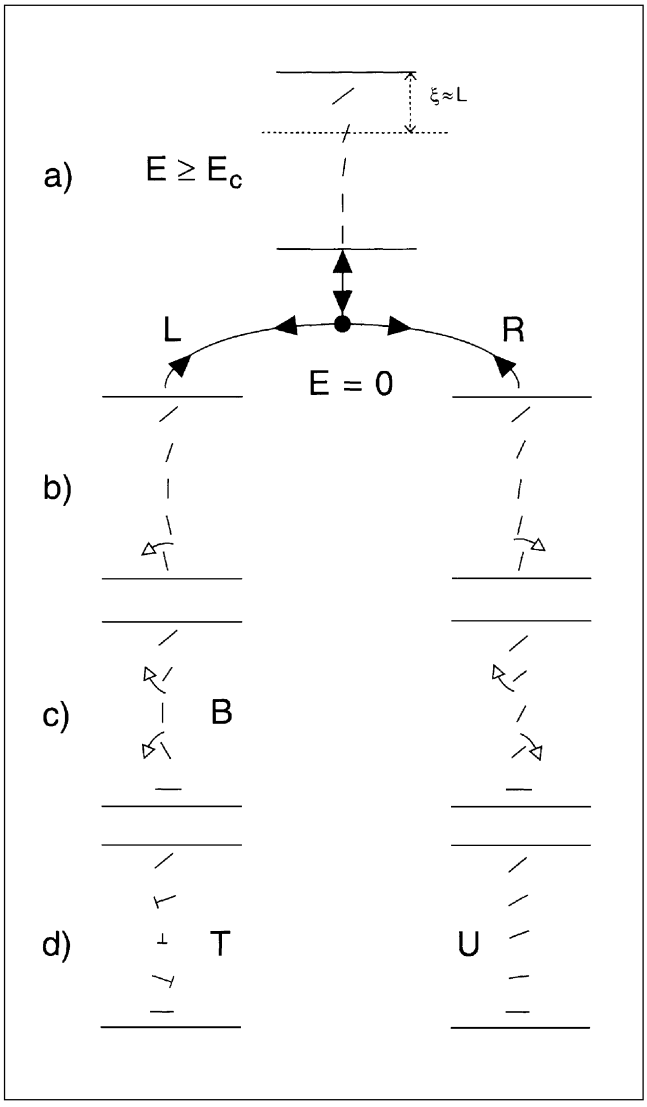


**Figure 4.** Switching by surface anchoring breaking. (**a**) $E > E_c$. Lower surface anchoring is broken. The initial state is forgotton. (**b**) $E = 0$. Relaxation towards $U$ or $T$. (**c**) After the surface relaxation time ($\sim 1\,\mu s$) the anchoring is 'healed'. The final texture is topologically blocked. Half-turn of bend-splay $B$ appears. (**d**) $B$ transforms into $T$, topologically equivalent.

off the field, the lower plate goes through the surface anchoring bifurcation point and the surface director $\mathbf{n}_l$ can rotate back toward its equilibrium planar orientation in two different ways: to the left (figure 4b, left) or to the right (figure 4b, right). Let us suppose for the time being that we can control the bifurcation, rotating slightly the director to the right or to the left. Once started, the rotation of $\mathbf{n}_l$ is accelerated by the exponentially

growing surface anchoring torque. After the surface relaxation time $\tau_s$, the anchoring on both surfaces returns to equilibrium (figure 4c) and the final surface state is 'written'. Calling $l\gamma$ the 'surface' viscosity [14] we expect $\tau_s$, defined as $\tau_s = \gamma l\, L/K$, to be in the range 1–10 μs, for our typical value $l \sim 100\,\text{Å} \ll L \sim 1000\,\text{Å}$. The bulk relaxes much slower, on the millisecond time scale for thin cells ($d \sim 1$ μm). In the right side scenario of figure 4, the sample relaxes continuously to the quasi uniform texture $U$. On the left side, a half-turn distortion is trapped in the sample from the beginning and cannot be resolved by continuous bulk deformation. The sample relaxes first to the half-turn bent state $B$. It then continuously transforms to the lower energy $\pi$-twisted state $T$, topologically identical.

Once relaxed (figure 4d), the textures $T$ or $U$ should remain stable in absence of a field. After a new application of field $E > E_c$, any one of these two textures can be brought back to the initial (figure 4a) state by breaking the anchoring and the switching can be repeated at will. Below $E_c$, the textures should stay unaffected.

## 5. Control of the switching

To control the bifurcation switching we use the coupling of the director between the two plates of the cell. Two different couplings exist, static and dynamic, and in both cases the strongly anchored upper plate ('master' plate) emits a 'command' signal, the broken anchoring 'slave' plate receives it and switches. As we shall show, the static coupling always produces the uniform state $U$ at the end of the command pulse, while the dynamic coupling always 'writes' the $T$ texture.

## 6. Static coupling

Let us decrease $E$ from $E_0 > E_c$ down to 0 slowly and continuously, avoiding any dynamic effects (figure 5). At the beginning $\xi < L$ and the slave plate anchoring is broken. Close to the 'unbroken' ($\theta = \theta_0$) master plate the bulk director is distorted. It relaxes exponentially down to the bottom plate with a small tilt of the order of $\Delta\theta_{\text{elast}} \approx \theta_0 \exp(-d/\xi)$ (figure 5a). For thin cells this elastically transmitted tilt is sufficient to lift the bifurcation degeneracy in the absence of other effects. When the field decreases slowly below $E_c$, the tilt increases keeping the same sign (figure 5b) and the sample relaxes always toward the quasi uniform $U$ state (figure 5c).

## 7. Dynamic coupling

Let us now turn off the field instantaneously at $t = 0$, starting again from $E_0 > E_c$. Close to the master plate the bulk director **n** rotates during the usual bulk relaxation time $\tau_s' = \gamma\xi^2/K$ back toward the equilibrium orientation $\theta_0$ (figure 6a). This rapid inhomogeneous rotation creates a surface flow $v \sim \xi/\tau_s'$. Note that $\tau_s' \sim 10$ μs is fast compared to the bulk relaxation time ($\sim \gamma d^2/K$), but remains slow compared with the vortex diffusion time $\tau_v$ through the thickness of the cell ($\tau_v = \rho d^2/\eta$, about 0.1 μs for $d \sim 1$ μm). During $\tau_s'$ a constant shear of the velocity gradient $V/d$ appears across the cell (figure 6a), and this creates a hydrodynamic torque on the slave plate equal to $\Gamma \sim \gamma l V/d \sim Kl/(Ld)$, since $\xi \approx L$. During the surface relaxation time $\tau_s$ this creates a surface tilt $\Delta\theta_{\text{hydro}} \approx l/d$,

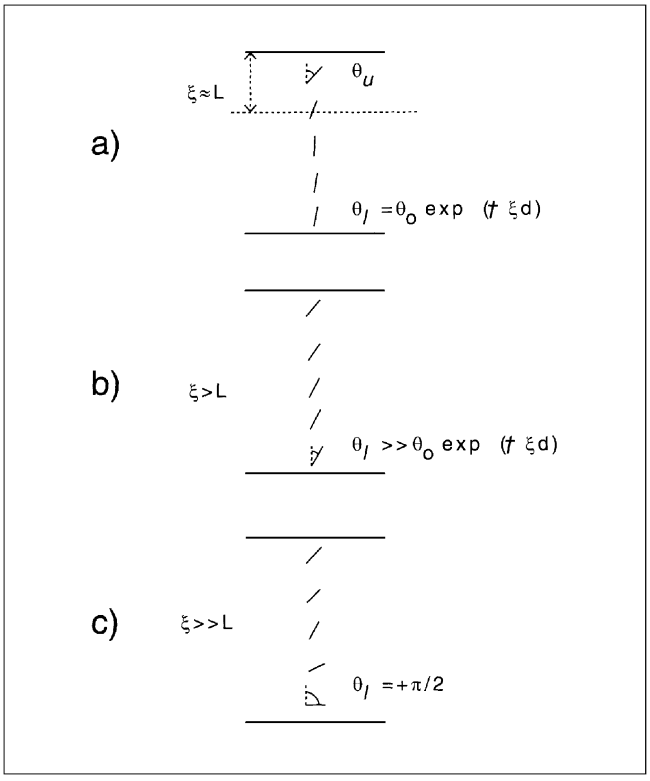


**Figure 5.** Elastic control of the bifurcation. (**a**) $E > E_c$. A small tilt remains on the lower plate, due to the elastic coupling with the upper plate. (**b**) At the bifurcation this small tilt is sufficient to lift the degeneracy. (**c**) The surface relaxation amplifies the initial tilt and leads to the $U$-state.

with a sign opposite to the elastic tilt $\Delta\theta_{\text{elast}}$ (figure 6b). For large $d/l$, (the usual situation), the hydrodynamic effect, decreasing like $1/d$, dominates over the exponentially decreasing elastic coupling, and one always obtains the final $T$ state.

## 8. Bifurcation control

To control the surface bifurcation one can use the balance between the elastic and the hydrodynamic couplings. If we turn off the field instantaneously, we always obtain the $B$ and $T$ textures, i.e. we 'write' the pixel. To 'erase', that is to produce the $U$ texture, one can simply slowly decrease the field. How slowly? Let us call $\tau$ the field decrease time, which now replaces $\tau_s'$. Comparing $\Delta\theta_{\text{elast}}$ with $\Delta\theta_{\text{hydro}}$ we estimate $\tau > \tau_s(L/d)\exp(d/L)$, giving $\tau > 1$ ms for $d \sim 1$ μm. To make the erasing pulses shorter, one can use a special form of the signal: a two-step decrease of the field, with a intermediate value adjusted to the static breaking threshold. The slave surface relaxation time becomes infinite and damps out most of the hydrodynamic effect.

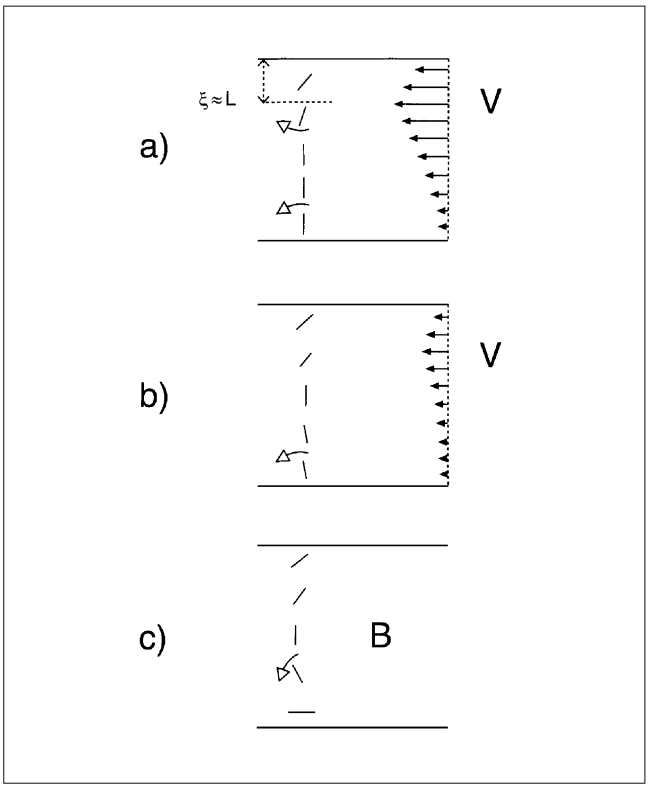


**Figure 6.** Dynamic control of the bifurcation. The field is switched off rapidly. (**a**) A surface flow $v$ is created at the upper plate by the rapid director rotation. It diffuses to the lower plate almost instantaneously. (**b**) The hydrodynamic torque, transmitted to the lower plate director, rotates it to the opposite side from figure 5. The cell goes to state $B$ (figure 4c, left) and $T$.

To summarize, the surface bifurcation behaves as an infinite gain mechanical amplifier. During the breaking of the surface anchoring a large potential energy is stored by the electric field in the broken anchoring. At the bifurcation, the system can, in principle, be controlled by command fields as small as we like.

## 9. Typical performances

We present some experimental results obtained with $4 \times 4$ pixel cells, giving an idea of the performance of the proposed display, e.g. speed, bistability, voltage thresholds and optical contrast. The detailed properties are presently controlled by several non-optimized important factors: the nature and strength of the anchorings, cell thickness, geometry of the cell, and the form of the driving signals.

For the slave plate we use simple planar (zero pretilt) anchoring with moderate strength, prepared by SiO oblique evaporation on ITO. The typical threshold field $E_c(\tau)$ needed for the anchoring breaking of the nematic 5 CB, is presented in figure 7 as a function of the

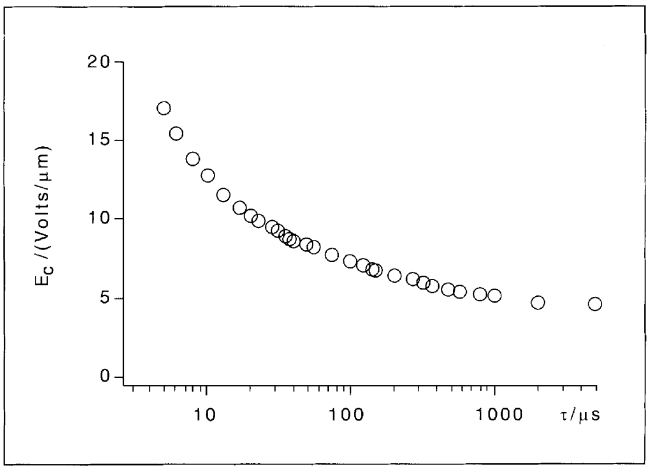


**Figure 7.** Dynamic anchoring breaking threshold for SiO aligned 5CB.

duration $\tau$ of an applied square electric pulse. The static threshold of about $5\,\mathrm{V\,\mu m^{-1}}$ corresponds to an extrapolation length $L \approx 450\,\text{Å}$. For short pulses the threshold increases, as already reported [10], but even for $\tau = 5\,\mu\mathrm{s}$ it remains compatible for thin cells with existing CMOS drivers ($V \approx 25\,\mathrm{V}$ for $d = 1.5\,\mu\mathrm{m}$). As expected, the threshold field $E_c$ does not depend on the cell thickness. The same behaviour of $E_c(\tau)$ is obtained for cell thicknesses ranging from $d = 0.5\,\mu\mathrm{m}$ to $d = 8\,\mu\mathrm{m}$. Similar results, apart from minor changes in the threshold field value, are obtained with opposite polarity of the field or applying a square-wave ac field.

The master plate in our samples has a strong tilted anchoring, obtained also by SiO evaporation. The typical cell thickness is $d \approx 1.5\,\mu\mathrm{m}$, defined by spherical spacers. To make the $U$ and $T$ textures bistable we dope the nematic 5CB with a few percent of a chiral material. When the natural pitch of the mixture is $p \approx 4d$, the energies of the $U$ and $T$ states become equal. During the filling of the sample we observe the random coexistence of large domains of $U$ and $T$ textures, which are found to be permanently bistable. We have checked that the system behaves as predicted. Each command pulse completely erases the previous state of the pixel and gives rise to the $U$ or $T$ state, depending on the shape of the pulse. The 64 μs video writing time, seen from figure 7, is obtained for $V \geq 12\,\mathrm{V}$ at $d = 1.5\,\mu\mathrm{m}$, and with 'bi-square' pulses one can erase with a similar voltage [9].

In figure 8 we show a few pixels of our sample, driven together in the uniform or in the twisted states. The sample is under crossed polarizers in a diagonal position. The $U$ state behaves as an optical retardation plate ($\sim \lambda/2$), giving maximum transmitted intensity (figure 8a). The half-turn twisted texture $T$ is far away from the wave-guiding regime and behaves almost as a isotropic (but chiral) optical system, introducing just a small rotation of the polarization $\sim 10^\circ$): under crossed polarizers $T$ is dark, almost black (figure 8b). Without optimization this gives an optical contrast of about 50 between the two bistable states.

In figure 9 we present the optical behaviour of the cell on a slow time scale. The sample is driven alternately into $U$ and $T$ by short pulses. Between the command pulses there is no visible change of the transmitted intensity, demonstrating the bistability of the pixel.

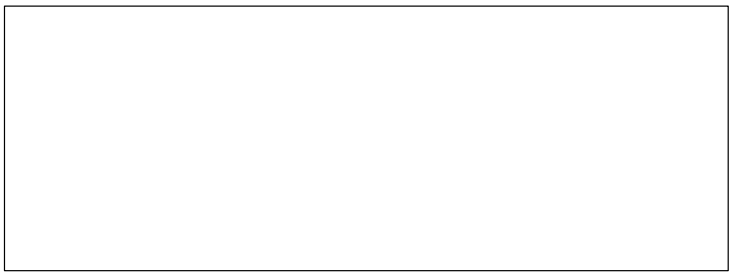

**Figure 8.** Photomicrograph of a few pixels of the sample, switched to the uniform (**a**) and to the twisted (**b**) states. The sample is under crossed polarizers in diagonal position.

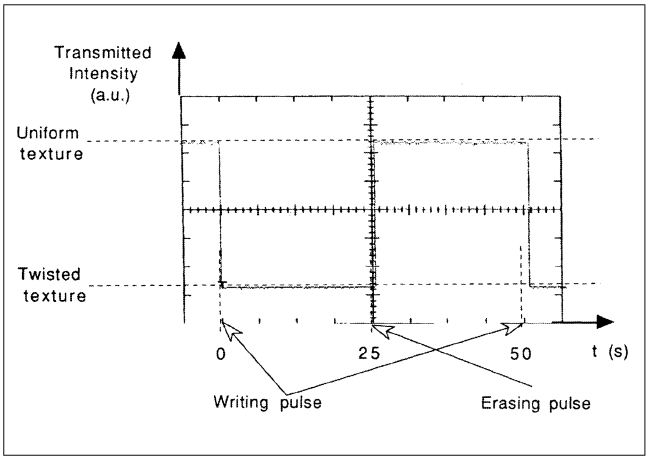


**Figure 9.** Optical bistability of the cell, written and erased by short pulses. For both textures there is no visible change of the intensity at this time scale.

## 10. Conclusion

It is now useful to compare the potentialities of the surface controlled bistable nematic display with other proposed bistable liquid crystal systems. The most advanced competitor is obviously the ferroelectric chiral smectic $C^*$ display [3]. Both systems need a control field in the same range and must use similar thin cells. Their comparable writing times (10–100 μs) are compatible with the line access time of a video matrix display. The optical response time of the nematic is slower (a few milliseconds), but still compatible with the video frame time. The big advantage of the nematic system is its large self-healing capability after mechanical shocks, compared to the shock sensitive $SmC^*$ device.

Two other nematic bistable devices have been demonstrated. The more advanced [15] is based on the Berreman [2] bulk $2\pi$-twist transition. In this case one goes continuously from one state to the other by a simple bulk distortion: this system is not topologically bistable, and another problem is its longer control time. A more recent nematic bistable device[16], using 'surface switching', presents texture bistability created above an aligning grating by the motion of surface defects. The optical contrast is not yet very large and

the switching time is at least two orders of magnitude slower than in our case. We do not discuss here the polymer stabilized bistable cholesteric systems, which work at higher voltages and are significantly slower.

The potential advantages of our nematic bistable display deserve further study for a better understanding of the mechanisms and better control of the material properties, in particular low cost surface treatments, long term stability, temperature range, and memory effects; these studies should stimulate further academic research. If their practical result is sufficiently positive, the surface controlled nematic bistable display could become industrially important and enter the restricted club of useful liquid crystal devices.

## Acknowledgement

This work was supported by Brite Euram contract no. BRE2-CT94-0614, by Esprit contract no. 25187 of the European Community and a CNRS-Sfim collaboration contract.

## References

[1] G D Boyd, J Cheng and P D T Ngo, *Appl. Phys. Lett*. **36**, 556 (1980)
[2] D W Berreman and W R Heffner, *Appl. Phys. Lett*. **37**, 109 (1980)
[3] N A Clark and S T Lagerwall, *Appl. Phys. Lett*. **36**, 899 (1980)
[4] R Barberi, M Giocondo and G Durand, *Appl. Phys. Lett*. **60**, 1085 (1992)
[5] G Durand, *Proc. SPIE*, **2949**, 2 (1996)
[6] I Dozov, M Nobili and G Durand, *Appl. Phys. Lett*. **70**, 1179 (1997)
[7] I Dozov, Ph. Martinot-Lagarde, E Polossat, I Lelidis, M Giocondo and G Durnad, *Proc. SPIE*, **3015**, 61 (1997)
[8] Ph. Martinot-Lagarde, I Dozov, E Polossat, M Giocondo, I Lelidis, G Durand, J Angele, B Pecout and A Boissier, *SID '97 Digest*, 41 (1997)
[9] G Durand, presented at the *VIIth International Topical Meeting on Optics of Liquid Crystals*, Heppenheim, to be submitted for publication (1997)
[10] A Gharbi, F R Fekih and G Durand, *Liq. Cryst*. **12**, 515 (1992)
[11] G Barbero and R Barberi, *J. Phys. (Paris)* **44**, 609 (1983)
[12] R Barberi and G Durnad, *Appl. Phys. Lett*. **58**, 2907 (1991)
[13] R Barberi, M Giocondo, J Li, R Bartolino, I Dozov and G Durand, *Proc SPIE*, **3013**, 229 (1997)
[14] E Virga and G Durand, presented at the *17th International Liquid Crystal Conference* (Strasbourg, 1998)
[15] T Tanaka, I Sato, A Inoue, Y Momose, H Nomura and S Lino, *Proceedings of Asia Display '95* (Tokyo, 1995) p. 259.
[16] E Wood and G P Bryan-Brown *et al*, presented at the *Network Meeting Liquid Crystals: Surface Properties from Basic to Application* (Moena, 1998)